Available online at www.sciencedirect.com
ScienceDirect
Acta Materialia 55 (2007) 5867–5872
Acta MATERIALIA
www.elsevier.com/locate/actamat

# Solute–vacancy binding in aluminum

C. Wolverton

*Northwestern University, Department of Materials Science and Engineering, Evanston, IL 60208, United States*

Received 27 December 2006; received in revised form 24 June 2007; accepted 25 June 2007
Available online 29 August 2007

**Abstract**

Previous efforts to understand solute–vacancy binding in aluminum alloys have been hampered by a scarcity of reliable, quantitative experimental measurements. Here, we report a large database of solute–vacancy binding energies determined from first-principles density functional calculations. The calculated binding energies agree well with accurate measurements where available, and provide an accurate predictor of solute–vacancy binding in other systems. We find: (i) some common solutes in commercial Al alloys (e.g., Cu and Mg) possess either very weak (Cu), or even repulsive (Mg), binding energies. Hence, we assert that some previously reported large binding energies for these solutes are erroneous. (ii) Large binding energies are found for Sn, Cd and In, confirming the proposed mechanism for the reduced natural aging in Al–Cu alloys containing microalloying additions of these solutes. (iii) In addition, we predict that similar reduction in natural aging should occur with additions of Si, Ge and Au. (iv) Even larger binding energies are found for other solutes (e.g., Pb, Bi, Sr, Ba), but these solutes possess essentially no solubility in Al. (v) We have explored the physical effects controlling solute–vacancy binding in Al. We find that there is a strong correlation between binding energy and solute size, with larger solute atoms possessing a stronger binding with vacancies. (vi) Most transition-metal 3d solutes do not bind strongly with vacancies, and some are even energetically strongly repelled from vacancies, particularly for the early 3d solutes, Ti and V.


*Keywords:* First-principles calculations; Solute–vacancy binding; Aluminum alloys

## 1. Introduction

Energetic binding between vacancies and solute atoms is a key factor in understanding diffusion [1,2]. The solute atoms themselves can obviously be directly influenced by a strong binding with vacancies, but solute–vacancy (hereafter, a vacancy is indicated by □) binding can also be a key influence on the solute diffusion of another species, e.g., by starving the diffusing species of vacancies. One example of the latter behavior can be seen in the observed decreased response of Al–Cu to natural aging with microalloying additions of Sn. This response is generally agreed to be connected with the idea of solute–□ interactions. Kimura and Hasiguti [3] first suggested that a strong Sn–□ binding energy could starve the diffusing Cu atoms of vacancies, thereby suppressing Cu clustering or GP zone formation, and hence the hardening effect of natural aging. This notion of strong solute–□ binding has subsequently been widely accepted to explain the effect of Sn, Cd and In on the decrease in natural aging response.

Given this connection between solute–□ binding and both diffusion and mechanical properties, many researchers have performed experiments aimed at obtaining values for these binding energies. Aluminum has often served as a prototypical solvent for these studies. Indeed, in a review of all references of solute–□ binding energies in Al up to ~1973, Mondolfo [2] quotes more than 100 different values for a large number of solute atoms. However, despite a long history of attempts to measure solute–□ binding energies, these bindings are notoriously difficult to measure accurately: the most notable case of contradictory experimental values is for Mg–□ binding. More than 20 values of this binding energy (see references in Refs. [1,2]) have

*E-mail address:* c-wolverton@northwestern.edu

1359-6454/$30.00 
doi:10.1016/j.actamat.2007.06.039

been reported in the literature, ranging from an extremely strong solute–□ binding of 0.4 eV to a very weak, but negative binding of −0.01 eV. (In this paper, we adopt the sign convention used in the literature, whereby positive binding energies indicate an energetically favorable binding.) Thus, in this case, even the sign of the binding is unclear. Values for other solute elements are not much better. For Cu–□ binding, the range of reported values is from 0 to 0.4 eV. Similar disparities exist for most other solute elements.

Fortunately, Balluffi and Ho [1] reviewed the status of this field (as of 1973), and critically assessed the experimental techniques used to deduce these binding energies. These techniques can roughly be divided into those relying on equilibrium experiments, and those relying on quenching experiments (see Ref. [1] and references therein for a discussion of these experimental techniques). The equilibrium experiments attempt to ascertain the equilibrium concentration of vacancies in a sample at thermal equilibrium either by combined length and lattice parameter measurements or positron annihilation experiments. Balluffi pioneered the use of combined length and lattice parameter measurements, and it is now generally acknowledged that these experiments provide the most reliable means to obtain vacancy concentrations. A large number of groups have performed quenching experiments, in which concentrations of quenched-in vacancies are determined (usually from electrical resistivity measurements), either as a function of temperature or with and without solute present. Balluffi and Ho [1] point out many sources of potential error in these quenching experiments, and demonstrate that these measurements often give erroneously large values for the binding energies. Thus, these authors argue that some of the apparent controversy between various experimental values in this field is simply due to the inaccuracies in many of the methods, and further argue that the values from equilibrium measurements are probably the most reliable. However, there are only a few such accurate measurements for the solute–□ binding in Al.

Here, we propose a new method – first-principles atomistic calculations – for obtaining solute–□ binding energies, and demonstrate that this is a reliable, quantitatively accurate and predictive method. In cases where Balluffi-type measurements exist, the first-principles values are in good agreement with them. However, we go beyond these few elements, and make a large database of predictions of these solute–□ bindings for a variety of solute elements, including practically all of the important alloying elements for commercial Al alloys. We also analyze the results of our calculations to search for the key physical effects which control the solute–□ binding.

## 2. First-principles methodology

The first-principles calculations described below utilize the plane wave pseudopotential method, as implemented in the Vienna ab initio Simulation Package (VASP), [4] using ultrasoft pseudopotentials [5,6]. For exchange correlation, we use both the local density approximation (LDA) of Ceperley and Alder [7,8] as well as the generalized gradient approximation (GGA) of Perdew and Wang [9]. Unless otherwise noted, all calculations are fully relaxed with respect to volume as well as all cell-internal and -external coordinates.

Convergence tests indicated that 237 eV (=17.5 Ry) was a sufficient cutoff to achieve highly accurate energy differences. Extensive tests of $k$-point sampling using equivalent [10] $k$-point meshes (using from $8\times8\times8$ to $32\times32\times32$ grids) indicated that an extremely dense grid of $k$-points is required for converged defect calculations in Al. We find that a $k$-point grid equivalent to a $24\times24\times24$ special-point grid in a face-centered cubic (fcc) structure is required for energetics to be converged to within 0.01 eV.

We have used defect supercells to obtain the energies of solute–□ pairs for various pair spacings. The binding energy is the energy of "infinite separation" minus nearest-neighbor separation. The "infinite separation" energy is given by two separate calculations performed with a single type of defect (either solute atom or vacancy). Specifically, for an fcc supercell with $N$ sites, the cell may contain no defects (with energy $E(\mathrm{Al}_N)$), may contain a vacancy ($E(\mathrm{Al}_{N-1}\square_1)$), a solute impurity ($E(\mathrm{Al}_{N-1}\mathrm{X}_1)$), or a solute–□ pair ($E(\mathrm{Al}_{N-2}\mathrm{X}_1\square_1)$). We calculate the binding energy from the combination of these four configurations via the following expression:

$$-E_{\mathrm{bind}}(\mathrm{X}\text{–}\square) = E(\mathrm{Al}_{N-2}\mathrm{X}_1\square_1) + E(\mathrm{Al}_N) - E(\mathrm{Al}_{N-1}\mathrm{X}_1) - E(\mathrm{Al}_{N-1}\square_1) \quad (1)$$

(The minus sign is to keep the binding energy consistent with the convention in the literature, with a positive binding energy indicating a favorable binding.) We note that by calculating the solute–□ binding energy from Eq. (1), one also can obtain easily as "byproducts" the dilute impurity energy

$$E_{\mathrm{imp}}(\mathrm{X}) = E(\mathrm{Al}_{N-1}\mathrm{X}_1) + \frac{N-1}{N}E(\mathrm{Al}_N) - E(\mathrm{X}) \quad (2)$$

and the vacancy formation energy

$$E_{\mathrm{vac}}(\square) = E(\mathrm{Al}_{N-1}\square_1) + \frac{N-1}{N}E(\mathrm{Al}_N) \quad (3)$$

For a more detailed discussion of recent first-principles calculations of impurity energies in Al, we refer the reader to Ref. [11].

In addition to energetics, the first-principles calculations also provide insight into the structure of the defects considered. To get a quantitative measure of the atomic size of each solute, we also compute the solute impurity volume for the solute X, $V^{\mathrm{X}}_{\mathrm{imp}}$, which is given by the volume change induced by placing a single solute impurity into pure Al:

$$V^{\mathrm{X}}_{\mathrm{imp}} = V(\mathrm{Al}_{N-1}\mathrm{X}_1) + V(\mathrm{Al}_N) \quad (4)$$

In all cases, bindings were calculated using supercells of both 32 and 64 atomic sites. (For simplicity, we refer to these as "32 atom" and "64 atom" cells, whether or not

they contain vacancies.) In many cases, the 32-atom cells produce results converged to within 0.01–0.02 eV with respect to 64-atom cells. However, for some transition metals, the errors are substantially larger; for a few of these cases, 128-atom cells were also tested. All results shown in this paper are for 64-atom supercells, unless otherwise noted. From the calculations of 128-atom supercells (see below), we suggest that the binding energies for 3d solutes are converged to within ±0.06 eV, and non-transition-metal solutes are converged significantly beyond this level, perhaps as low as ±0.01 eV.

## 3. Results

### 3.1. Validating the first-principles binding energies

We begin by comparing our first-principles calculated bindings for elements where accurate measurements exist. Our calculated results for solutes Mg, Cu, Ag, Zn and Si are given in Table 1, along with the most reliable experimental values. Only experimental values critically assessed by Balluffi and Ho [1] to be reliable are shown. These experimental values are all taken from equilibrium experiments: all results are from combined length and lattice parameter measurements, except for the Zn-binding energy for which no such measurement exists (the quoted value comes from positron annihilation measurements). In each case, there is a good agreement between theory and experiment, particularly in the case of Mg, for which a negative binding energy is calculated, consistent with the Balluffi-type experiments, but in contrast to the early reports of a large Mg–□ binding energy deduced from quenching experiments. Thus, we conclude from this comparison that first-principles calculations of the type performed here are capable of quantitatively accurate predictions of solute–□ binding energies. Having developed confidence in the accuracy of the method, we next turn to binding energies for solute atoms for which experimental data is not available.

Table 1
Comparison of experimental and calculated solute–□ binding energies in Al

| Solute–vacancy pair | Measured value (eV) | First-principles value (eV) (present work) |
|---|---|---|
| Cu–□ | $0.00 \pm 0.12$ | ∼0.02 |
| Mg–□ | $-0.01 \pm 0.04$ | −0.02 |
| Si–□ | 0.03 | 0.08 |
| Zn–□ | 0.02 | 0.03 |
| Ag–□ | 0.05 | 0.07 |

Of the large number of reported energies, only experimental values critically assessed by Balluffi and Ho [1] to be reliable are shown. These experimental values are all taken from equilibrium experiments: all results are from combined length and lattice parameter measurements, except for the Zn- binding energy for which no such measurement exists (the quoted value comes from positron annihilation measurements). First-principles results are from fully-relaxed, VASP (64-atom) supercell calculations. All first-principles results are using LDA, with the exception of Si, which is GGA. The agreement between theory and experiment is quite good, and well within the uncertainty of the two methods, demonstrating that these calculations provide quantitatively accurate predictions of solute–□ binding energies.

### 3.2. Solute–vacancy binding of microalloying additions to Al–Cu: Sn, In, Cd, Ge and Si

Next, we wish to analyze the effect of microalloying of Sn, In and Cd in Al–Cu alloys mentioned in the Introduction. We wish to ascertain whether our results support solute–□ binding explaining the observed decrease in natural aging response with these microalloying additions. For the microalloying additions Sn, In and Cd, Baluffi-type measurements are not available for the solute–□ bindings. On the other hand, quenching experiments have been performed for Sn–□, In–□ and Cd–□ binding, yielding relatively large values. These large binding energies would seem to confirm the suspected mechanism for reduced natural aging of microalloyed Al–Cu alloys. However, since these quenching experiments are known to sometimes give erroneously large binding energies, accurate values of these binding energies are not available. Hence, confirmation of the proposed solute–□ mechanism is still lacking.

Table 2
First-principles solute–vacancy (□–X) binding energies in Al

| Solute | Solute–vacancy $\delta E_b^{\square-X}$ | |
|---|---|---|
| | NN | 2NN |
| Mg-64 | −0.02 | −0.01 |
| Si(GGA)-64 | 0.08 | 0.02 |
| Sc-64 | −0.17 | 0.05 |
| Ti-64 | −0.35 | 0.04 |
| V-64 | −0.33 | 0.05 |
| Cr(LDA)-64 | −0.25 | 0.05 |
| Cr(GGA)-64 | −0.22 | 0.06 |
| Mn(GGA)-64 | −0.08 | 0.08 |
| Fe(GGA)-64 | ∼0 | 0.08 |
| Co(LDA)-64 | 0.02 | 0.04 |
| Co(GGA)-64 | 0.04 | 0.06 |
| Ni(LDA)-64 | 0.03 | 0.03 |
| Cu(LDA)-64 | 0.02 | 0.02 |
| Cu(GGA)-64 | 0.04 | |
| Zn-64 | 0.03 | −0.01 |
| Ga(LDA)-64 | 0.07 | −0.01 |
| Ga(GGA)-64 | 0.09 | 0.01 |
| Ge(GGA)-64 | 0.13 | ∼0 |
| Sr-64 | 0.72 | 0.01 |
| Zr-64 | −0.28 | 0.05 |
| Ag-64 | 0.07 | ∼0 |
| Cd-64 | 0.14 | −0.02 |
| In-64 | 0.20 | −0.04 |
| Sn-64 | 0.25 | −0.03 |
| Sb-64 | 0.30 | −0.04 |
| Ba-64 | 1.42 | |
| Au-64 | 0.15 | ∼0 |
| Pb-64 | 0.41 | −0.05 |
| Bi-64 | 0.44 | −0.06 |

Given are binding energies for 64-atom cells, for both nearest-neighbor and second-nearest-neighbor solute–□ pairs. Energies are in eV/defect pair. Positive energies indicate energetically favorable binding. Results are for $24 \times 24 \times 24$ equivalent $k$-point grids. Unless otherwise noted, calculations are performed using the LDA.

Table 2 gives the first-principles calculated values for solute–□ binding for all solutes considered in this work. Both nearest-neighbor (NN) and second-neighbor (2NN) bindings are given. For some solute elements, we compare results for both LDA and GGA exchange correlations. Our first-principles results in Table 2 show the NN □-binding energies of Sn, In and Cd to be quite large: 0.25, 0.20 and 0.14 eV, respectively. These values are all very large compared with that of Cu (0.02 eV), lending compelling evidence to the proposed solute–□ binding mechanism for the natural aging response.

In addition, these calculations provide a prediction that Ge, and to a lesser extent Si, give a fairly large vacancy binding energy as well, 0.13 and 0.08 eV, respectively. This is interesting in light of the very recent reports [12,13] that particles of Ge and Si in Al–Cu alloys can "catalyze" the precipitation of $\theta'$ in an analogous manner to that of Sn. Our results suggest that Si and Ge additions should also decrease the natural aging response in Al–Cu, a prediction awaiting experimental confirmation.

We note that Hashimoto and Ohta [14,15] measured the solute–□ binding for several solutes relative to that of Zn by examining the kinetic response of Al–Zn alloys to aging with and without the solute atoms present. Although these types of non-equilibrium experiments may contain sources of error for the precise quantitative values of the binding energy, one should still be able to compare the trends in binding between various solutes. It is interesting to note that the observed trends in kinetic aging response for the solutes examined suggested the following relative order of binding energies: Si < Cd ~ Ge < In < Sn. This is precisely the relative ordering that we determined from our first-principles calculations (Table 2).

We also note that our calculations show that Au has a sizeable binding energy with vacancies (0.15 eV), suggesting a similar effect for microalloying additions of Au. To our knowledge, microalloying Au in Al–Cu alloys has not been attempted, but an experimental test of this prediction would be most interesting.

### 3.3. Physical contributions to solute–vacancy binding in Al

#### 3.3.1. Solute size

We next analyze the general trends and physical factors controlling binding across all solutes. We begin with a discussion of the effect of solute size. Fig. 1 shows the calculated NN binding energies as a function of the solute impurity volume, given by Eq. (4). There is a correlation between solute–□ binding and size of the impurity atoms, with larger solutes having a larger binding energy with vacancies. If one excludes the 3d transition metals (Sc–Zn, connected by dashed lines) from Fig. 1, the correlation is particularly clear. From this plot, one can see that the large binding energies for the microalloying additions Sn, In and Cd are clearly due to their large sizes compared to Al.

In addition to the large binding energy of Sn, In and Cd, we predict other solute elements possessing even higher

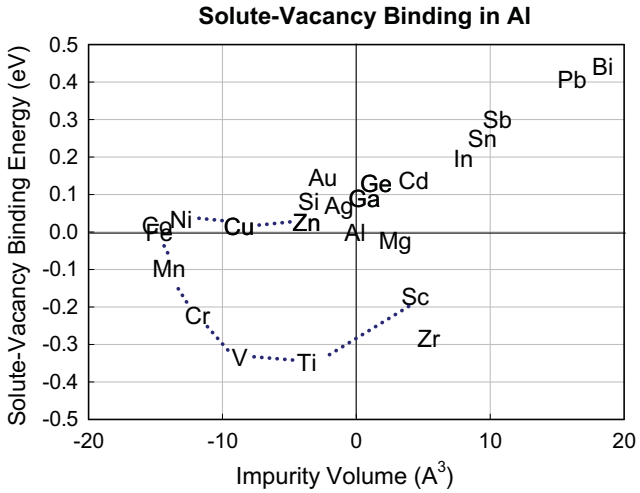


Fig. 1. First-principles calculated nearest-neighbor solute–□ binding energies as a function of the solute impurity volume. The impurity volume is calculated from the change in volume upon adding a single solute impurity to pure Al [Eq. (4)]. Note the correlation between solute–□ binding and size of the impurity atoms, with larger solutes having a larger binding energy with vacancies. The correlation is particularly clear if one excludes the 3d transition metals, Sc–Zn, connected by dashed lines.

binding energies with vacancies: Pb (0.41 eV), Bi (0.44 eV), Sr (0.72 eV) and Ba (1.42 eV). These remarkably large binding energies are due to the fact that these impurities have extremely large volumes. However, the extremely large atomic sizes of these impurities yields extremely large strains, and hence very unfavorable dilute impurity energies. Thus, in all of these cases, these very large impurities possess virtually no solubility in Al. It is noteworthy that additions of Pb and Bi do not yield the same effect on Al–Cu as Sn [5,6], presumably due to their lack of solubility in Al.

Also, other trends emerge from Fig. 1: By comparing isoelectronic sets of solutes (i.e., solutes in the same column of the periodic table, Cu/Ag, Zn/Cd, Si/Ge/Sn), one can see a clear trend that larger atoms tend to bind more strongly with vacancies. Comparing solutes in the same row of the periodic table (Ag/Cd/In/Sn) one also observes the same trend: the larger the atom, the stronger the binding. This simple observation also fits with the very large binding energies of the insoluble elements: Ba is the largest solute atom considered, with Sr being the second largest considered.

The correlation between solute–□ binding and solute size may be understood by a simple physical argument: Placing large impurity atoms in an Al matrix induces a significant strain on the surrounding Al atoms. A vacancy next to this large impurity allows the impurity to relax towards the vacancy and hence away from the other neighboring Al. Thus, the vacancy in a NN position to a large impurity helps to relieve the strain, producing an energy lowering of the X–□ pair, and hence a stronger binding energy. However, we note below that, in addition to simple strain relief, there is also an important electronic aspect to this size effect.

There are exceptions to the size-effect rule: Au, Si and Ag have a negative impurity volume (indicating that they are smaller than Al as a dilute impurity), but still have strong binding energies. Furthermore, Mg is notable as a large impurity that has no binding energy with vacancies. Hence, though solute size is a large factor in controlling the binding, it is clearly not the only factor.

Fig. 2 shows the 2NN solute–□ binding vs. solute impurity volume. In general, the 2NN binding energies tend to be fairly small, generally much smaller in magnitude than the NN binding energies. There is a slight negative correlation between 2NN binding and impurity volume.

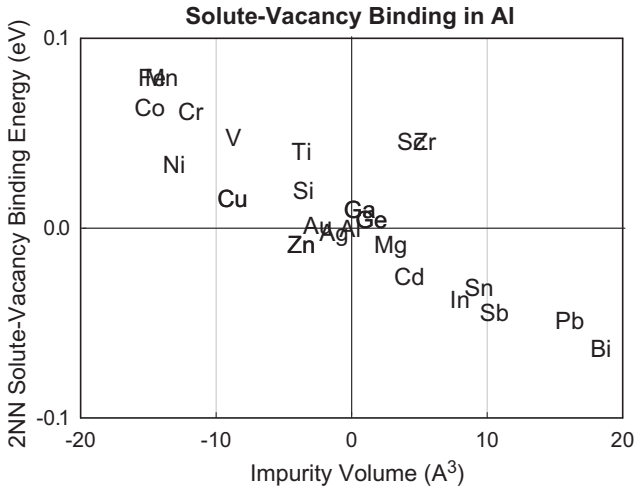


Fig. 2. First-principles calculated 2NN solute–□ binding energies as a function of the solute impurity volume. The impurity volume is calculated from the change in volume upon adding a single solute impurity to pure Al [Eq. (4)].

### 3.3.2. Binding with 3d transition metal solutes

From Fig. 1, it is clear that the solute size effects alone cannot explain the binding energies across the 3d series. Fig. 3 shows the calculated NN and 2NN binding energies across the 3d series. There is a clear trend across this series, with either negative or very small positive NN binding energies for all 3d solutes. The negative NN binding energies are most pronounced near the beginning of the 3d series, with Ti and V having the largest repulsive interaction with vacancies (for the most accurate calculations, labeled "Relaxed (64 atom)"). The 2NN binding energies are generally small, but positive across the series (again, for "Relaxed (64 atom)").

There is a previous first-principles calculation of solute–□ binding in Al, which specifically focused on the binding across the transition metal series [16]. These authors have pointed out that the trend in binding across the 3d series may be understood in terms of the strong bonding between 3d solutes and Al: since these solutes form very strong Al—X bonds, it is unfavorable for a solute atom to be placed near a vacancy, since this will result in fewer Al—X bonds.

Although this previous study [16] identifies many interesting qualitative trends, these authors did not account for atomic relaxation in their calculations. Given the above identification of strain and solute size as a primary factor, we wished to ascertain the role of atomic relaxation on binding energies. Fig. 3 shows the binding energies calculated in an "unrelaxed" geometry (i.e., with all atoms precisely constrained to the sites of a perfect fcc Al lattice),

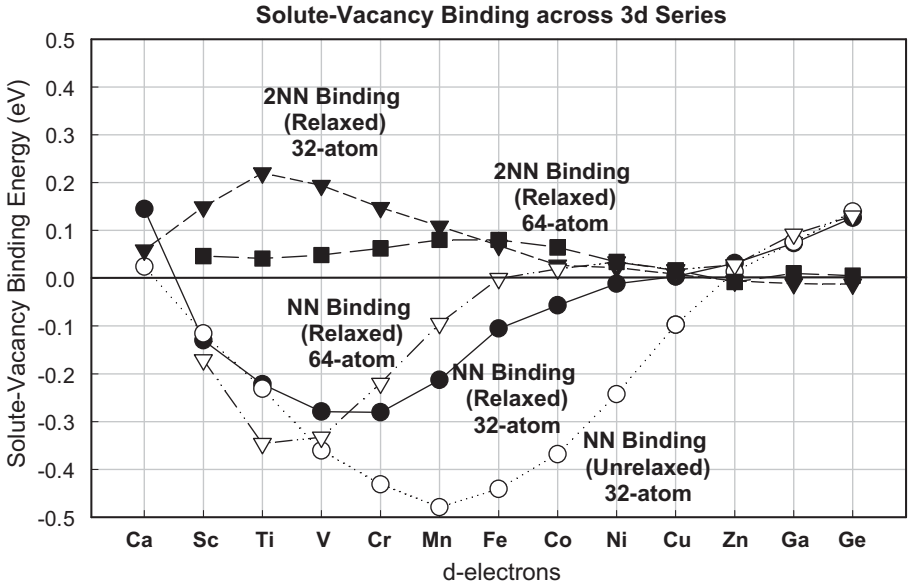


Fig. 3. First-principles calculated solute–□ binding energies across the 3d series. Shown are the 32-atom results, both for atomically relaxed as well as "unrelaxed" geometries (where all atoms are on ideal fcc lattice sites).

Table 3
Nearest-neighbor (NN) solute–□ binding energies computed as for different supercell sizes: 32-atom, 64-atom and 128-atom

| Solute | Solute–vacancy binding | | |
|---|---|---|---|
| | 32-atom | 64-atom | 128-atom |
| Ti | −0.22 | −0.35 | −0.30 |
| Fe (GGA) | −0.10 | ∼0 | +0.06 |
| Mn (GGA) | −0.20 | −0.08 | −0.02 |
| Mg | ∼0 | −0.02 | −0.03 |

Included are three 3d elements (Ti, Fe, Mn) and one non-transition-metal solute (Mg). The results for Ti and Mg are calculated using LDA, and Fe and Mn are calculated using GGA.

compared with the "relaxed" calculations, in which atoms are moved off ideal fcc positions to their zero-force positions. Our calculations of the "unrelaxed" binding energies agree very well with the previous calculations of Hoshino [16]. By comparing the curves of "Relaxed 32-atom" with "Unrelaxed 32-atom" in Fig. 3, we can ascertain the effect of atomic relaxation. Although the overall trend of binding in Fig. 3 is not severely affected by relaxation, it can be quantitatively important. The "unrelaxed" calculations show a significantly more negative binding, with the largest negative value for Mn, whereas, the relaxed calculations move the largest negative binding to earlier in the 3d series.

### 3.3.3. Effects of supercell size

In Fig. 3, we also show the comparison between binding calculated with 32-atom and 64-atom cells. We find that for these transition metals, there is a significant effect of cell-size on the binding energies, but for non-transition-metal solutes, this cell-size effect is much smaller. We also note that further distances between solutes and vacancies (2NN binding) yield an even stronger effect on cell-size. (For the 32-atom cells, the 2NN bond is already half-way across this supercell, so it is not too surprising that 2NN defect pairs are more sensitive to cell size, and the 32-atom results are not converged.) For three solutes that have NN binding most sensitive to cell size (Ti, Fe and Mn), we have also computed the binding energies using 128-atom supercells. For comparison, we have also performed 128-atom calculations for one non-transition-metal solute, Mg. These results are given in Table 3. It is clear from these results that the transition metals show a large dependence on supercell size. For Fe, even the sign of the binding energy changes in going from 32-atom to 128-atom calculations. For these three 3d solutes, it appears that the 128-atom calculations are converged to within approximately ±0.06 eV relative to the 64-atom results. Hence, this should probably be considered the size of the uncertainty for the quoted binding energies for 3d solutes. In contrast, the binding in Mg is much less sensitive to cell size, and the 128-atom and 64-atom results differ by less than 0.01 eV. Thus, we suggest that the uncertainty in binding energies for the non-transition-metal solutes quoted in Table 2 is much lower than that of transition metal solutes, perhaps as low as ±0.01 eV.

## 4. Summary

In summary, we have shown that first-principles calculations are capable of producing quantitatively accurate solute–□ binding energies in Al. For solutes where there are accurate experimental measurements, the calculated values agree with the measurements. This agreement gives us confidence in the predicted values for which no experimental measurements exist. Thus, we assert that some previously reported large binding energies (e.g., for Cu and Mg) are erroneous, as these solutes show either very weak, or even repulsive, binding energies.

Large binding energies are found for Sn, Cd and In, confirming the proposed mechanism for the reduced natural aging in Al–Cu alloys containing microalloying additions of these solutes. In addition, we predict that similar reductions in natural aging should occur with additions of Si, Ge and Au, and hope that experiments will be performed to test these predictions. Even larger binding energies are found for other solutes (e.g., Pb, Bi, Sr, Ba), but these solutes possess essentially no solubility in Al.

We have explored the physical effects controlling solute–□ binding in Al. We find that there is a strong correlation between binding energy and solute size, with larger solute atoms possessing a stronger binding with vacancies. This size effect is understood in terms of a strain-relief argument, whereby the strain associated with large solute atoms may be partially relieved by a neighboring vacancy.

For transition metal solutes in the 3d series, solute size does not fully explain the binding, and electronic structure band filling effects play a significant role as well. For the most part, 3d solutes do not bind strongly with vacancies, and some are even energetically strongly repelled from vacancies, particularly for the early 3d solutes, Ti and V.

## References

[1] Balluffi RW, Ho PS. In: Diffusion metals park. OH: Am Soc Metals; 1973. p. 83.
[2] Mondolfo LF. Aluminum alloys: structure and properties. London: Butterworth; 1976.
[3] Kimura H, Hasiguti RR. Acta Met 1961;9:1076.
[4] Kresse G, Hafner J. Phys Rev B 1993;47:558;
G. Kresse, Thesis, Technische Universität Wien, 1993;
Kresse G, Furthmüller J. Comput Mat Sci 1996;6:15;
Kresse G, Furthmüller J. Phys Rev B 1996;54:11169.
[5] Vanderbilt D. Phys Rev B 1990;41:7892.
[6] Kresse G, Hafner J. J Phys.: Condens Mat 1994;6:8245.
[7] Ceperley DM, Alder BJ. Phys Rev Lett 1980;45:566.
[8] Perdew JP, Zunger A. Phys Rev B 1981;23:5048.
[9] Perdew JP. In: Ziesche P, Eschrig H, editors. Electronic structure of solids 1991, vol. 11. Berlin: Akademie Verlag; 1991.
[10] Froyen S. Phys Rev B 1989;39:3168.
[11] Wolverton C, Ozoliņš V. Phys Rev B 2006;73:144104.
[12] Mitlin D, Radmilovic V, Morris Jr JW. Metal Mat Trans 2000;31A:2697.
[13] Mitlin D, Radmilovic V, Dahmen U, Morris Jr JW. Metal Mat Trans 2001;32A:197.
[14] Hashimoto F, Ohta M. J Phys Soc Jpn 1964;19:1331.
[15] Ohta M, Hashimoto F. J Phys Soc Jpn 1964;19:1987.
[16] Hoshino T, Zeller R, Dederichs PH. Phys Rev B 1996;53:8971.